

High-Fidelity Workshop Scitech 2022: RANS SA-[neg]-QCR2000 Joukowski Airfoil Case

Marshall Galbraith
galbramc@mit.edu

January 19, 2021

1 Introduction

This test case is designed as a verification case of the turbulence model of the SA-[neg]-QCR2000 RANS equations. Participants are required to use the provided grids as they are designed so the optimal convergence rate in drag coefficient error can be observed. For adjoint consistent discretizations, the theoretical optimal convergence rate in drag error is $2P$ (though it has been observed with schemes that lack adjoint consistency), where P is the polynomial degree of the discretization. Without adjoint consistency, the expected drag error convergence rate is $P + 1$. The Joukowski airfoil is used for this test as the cusped trailing edge removes the inviscid singularity at the trailing edge at zero degrees angle of attack. However, there is still a singularity in skin friction. The provided grids are design to cluster nodes at both the trailing edge singularity and the stagnation point in order to capture the expected order of accuracy. Please do not hesitate contact Marshall Galbraith as soon as possible if you are having difficulties using the provided grids.

2 Governing Equations and Models

The compressible Reynolds Averaged Navier-Stokes equations should be used with air as the working medium. The freestream Mach number is 0.5, the Reynolds number is 1,000,000 based on chord, the angle of attack is 0 degrees, and the heat capacity ratio is $\gamma = Cp/Cv = 1.4$. The Prandtl number is fixed to $Pr = 0.72$, and a turbulent Prandtl number of $Pr_t = 0.9$. The dynamic viscosity is determined by Sutherland's law:

$$\mu(T) = \mu_0 \left(\frac{T}{T_0} \right)^{3/2} \left(\frac{T_0 + S}{T + S} \right) \quad (1)$$

where $\mu_0 = 1.716 \times 10^{-5} \text{ kg/(ms)}$, $T_0 = 491.6^\circ \text{ R}$, $S = 198.6^\circ \text{ R}$. In a non-dimensional form, normalized by μ_{ref} and $T_{ref} = 520^\circ \text{ R}$, Sutherland's law is:

$$\frac{\mu(T)}{\mu_{ref}} = \left(\frac{T}{T_{ref}} \right)^{3/2} \left(\frac{1 + S/T_{ref}}{T/T_{ref} + S/T_{ref}} \right) \quad (2)$$

Participants should use a freestream value $\nu_t/\nu = 3$ for the SA-[neg]-QCR2000 turbulence model.

Participants must use the SA-QCR2000 turbulence model of Spalart (2000) or the the equivalent "negative-SA"¹ by Allmaras *et al.* (2012) with the QCR2000 terms, e.g. SA-neg-QCR2000.

¹http://www.iccfd.org/iccfd7/assets/pdf/papers/ICCFD7-1902_paper.pdf

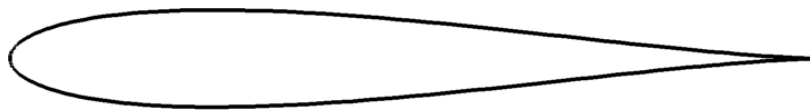


Figure 1: Joukowski airfoil geometry.

Because this will have a significant effect on the “truth” drag coefficient value, the turbulence model must be carefully documented. We strongly recommend the use of test cases from the NASA Turbulence Modeling Resource (<http://turbmodels.larc.nasa.gov/>) web site to verify correct implementation of the turbulence model, where details of the mathematical formulation for the SA-[neg]-QCR2000^{2 3} model are also available

3 Meshes

A set of Python scripts are provided that can generate both quadrilateral and triangular grids that are exported in a variety of file formats. Two families of meshes are available: The **Classic** family of meshes uses the Joukowski conformal map directly to generate the grid and produces nearly perfectly orthogonal elements and were used in the AIAA Paper 2021-1552. The **Challenge** set of meshes produces meshes with higher degrees of skew near the wall which can degrade the solution quality for some discretizations. There is also an option to generate high-order curved grids. The main script to generate the grids is `Joukowski_Mesh.py`, which contains options for the grid polynomial degree, the grid family, the number of refinement levels, and the desired grid format.

4 Boundary Conditions

The far field boundary can be imposed with a Riemann invariant or characteristic boundary condition. Note that the far field boundary is not far enough away to be completely non-influential. Hence the boundary condition used must be documented, and will likely lead to slight difference in the “truth” drag coefficient on the finest mesh. The airfoil surface is imposed as a no-slip adiabatic wall.

5 Common Inconsistencies

The following is a list of common inconsistencies that can lead to computing a different “truth” drag coefficient value.

1. Using a different Prandtl number than 0.72.
2. Using constant viscosity rather than Sutherland’s law.
3. Using isothermal wall rather than adiabatic wall.
4. Using modified SA turbulence models will have a significant effect.
5. Using a freestream value other than $\nu_t/\nu = 3$.

²<https://turbmodels.larc.nasa.gov/spalart.html#sa>

³<https://turbmodels.larc.nasa.gov/spalart.html#qcr2000>

6 Mandatory Campaign

The main objective is to demonstrate grid convergence of drag coefficient error on a sequence of successively refined meshes. The provided meshes must be used for all calculations. Participants should provide a non-dimensional drag coefficient error for each of the grids. Due to variations in boundary condition implementations, participants should compute a reference drag coefficient on the finest grid with the highest order of accuracy available in their software. The drag coefficient error for each grid is computed relative to this reference drag coefficient. Participants should also verify that machine zero lift is computed on all grids.

1. Start the simulation from a uniform free stream with $M = 0.5$ everywhere, and monitor the L^2 -norm of the density residual. Optionally compute the work units required to achieve a steady state where the density residual has dropped at least 10 orders of magnitude.
2. Perform this exercise for at least four different meshes and with different orders of accuracy to assess the performance of schemes of various accuracy.
3. Plot the drag coefficient error vs. work units to evaluate efficiency, and drag coefficient error vs. length scale to assess the numerical order of accuracy.
4. The raw data should be provided in three columns, DOF, drag coefficient, and work units (work units are optional). The data should be separated by different P values. An example format is provided below:

P = 0

DOF	Cd	Work Units (optional)
xxx	xxx	xxx
xxx	xxx	xxx

P = 1

DOF	Cd	Work Units (optional)
xxx	xxx	xxx
xxx	xxx	xxx

7 Presentation Guideline

Participants verification slide should include a plot of the order of accuracy that includes the reference slope lines as illustrated in the figure below. These slope lines provide a consistent reference across all presentations. The data for the slopes are given below, and provided in a tecplot format on the website. Please use either the P+1 or 2P slopes depending on the expected order of accuracy of the scheme.

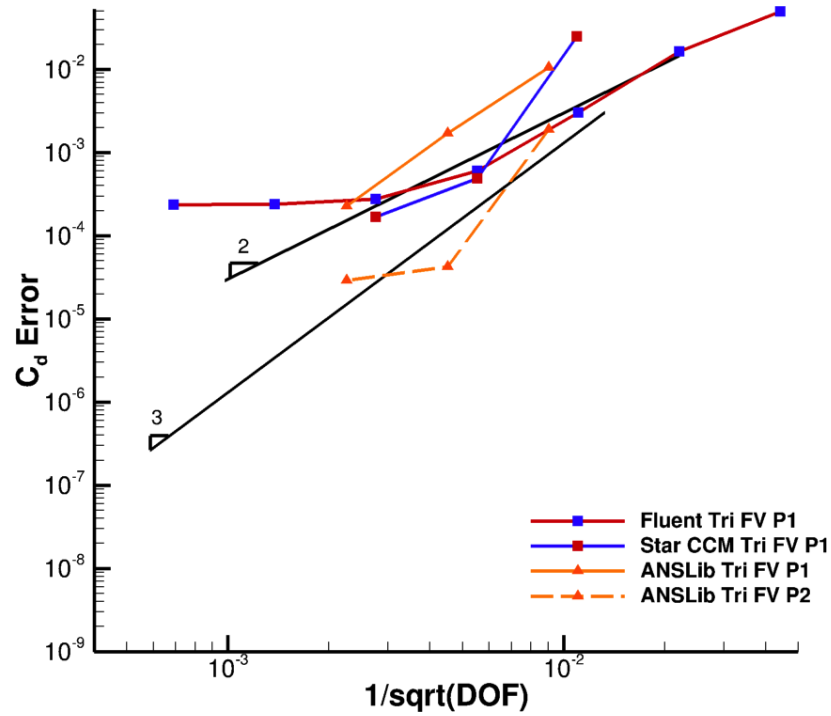


Figure 2: Example order of accuracy plot that includes P+1 reference slope lines.

Reference slope lines for P+1 slopes

P=1 Slope of 2

1/sqrt(DOF)	Cd Error
0.0220970869	1.47E-002
0.0009765625	2.86892231708631E-05

P=2 Slope of 3

1/sqrt(DOF)	Cd Error
0.0132582521	3.02E-003
0.0005859375	2.6056752059198E-07

P=3 Slope of 4

1/sqrt(DOF)	Cd Error
0.0147313913	2.31E-003
0.0006510417	8.80994128638802E-09

P=4 Slope of 5

1/sqrt(DOF)	Cd Error
0.0099436891	4.93E-004
0.0012429611	0.000000015

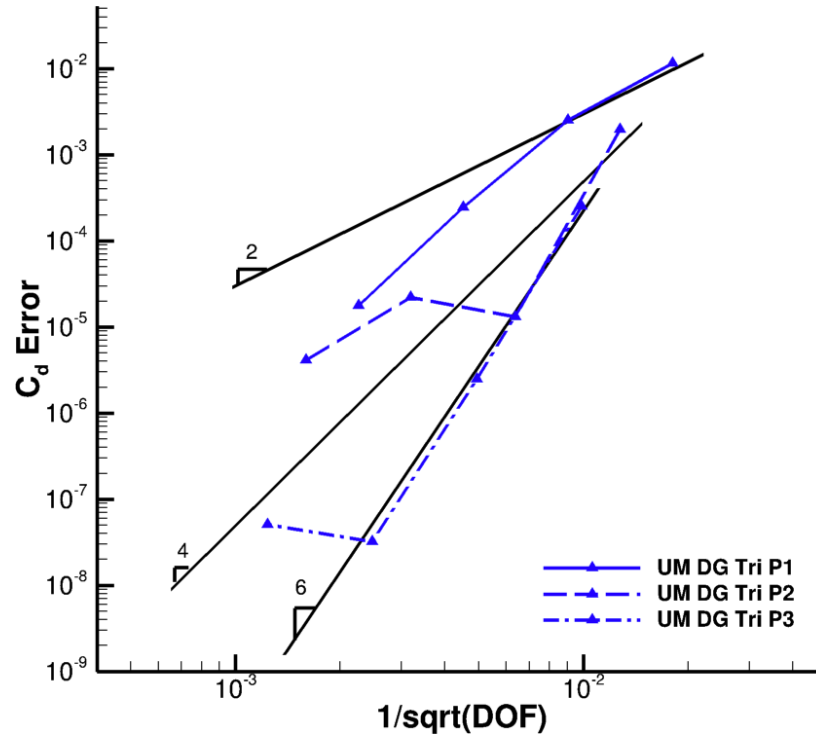


Figure 3: Example order of accuracy plot that includes 2P reference slope lines.

Reference slope lines for 2P slopes

P=1 Slope of 2

1/sqrt(DOF)	Cd Error
0.0220970869	1.47E-002
0.0009765625	2.86892231708631E-05

P=2 Slope of 4

1/sqrt(DOF)	Cd Error
0.0147313913	2.31E-003
0.0006510417	8.80994128638802E-09

P=3 Slope of 6

1/sqrt(DOF)	Cd Error
0.0110485435	4.07E-004
0.0013810679	1.55210937485436E-09

P=4 Slope of 8

1/sqrt(DOF)	Cd Error
0.0088388348	2.90E-005
0.0022097087	4.41862957464893E-10

References

- ALLMARAS, STEVEN R., JOHNSON, FORRESTER T. & SPALART, PHILIPPE R. 2012 Modifications and clarifications for the implementation of the spalart-allmaras turbulence model. Seventh International Conference on Computational Fluid Dynamics. Big Island, Hawaii.
- SPALART, P. R. 2000 Strategies for turbulence modelling and simulation. *International Journal of Heat and Fluid Flow* **21**, 252–263.